Structural states of Mg cordierite. IV. Raman spectroscopy and local order parameter behaviour

1990 J. Phys.: Condens. Matter 2 6361

(http://iopscience.iop.org/0953-8984/2/30/002)

J. Phys.: Condens. Matter 2 (1990) 6361–6372. Printed in the UK

Structural states of Mg cordierite: IV. Raman spectroscopy and local order parameter behaviour

Wilson C-K Poon†§, Andrew Putnis† and Ekhard Salje‡

† Cavendish Laboratory, University of Cambridge, Madingley Road, Cambridge CB3 0HE, UK

‡ Department of Earth Sciences, University of Cambridge, Downing Street, Cambridge CB2 3EQ, UK

Received 17 January 1990

Abstract. The time evolution of Al–Si ordering and ferroelastic distortion in isothermally annealed Mg cordierite ($Mg_2Al_4Si_5O_{18}$) is studied using Raman spectroscopy. The transition from the initial hexagonal to the modulated structure is found to be discontinuous, with the quenched modulated structure being locally orthorhombic. The bilinear coupling between Al–Si ordering and lattice distortion proposed previously to account for observed behaviour in the macroscopically orthorhombic phase obtained after prolonged annealing is shown to be also valid on a local scale in the modulated phase. Modes of the hexagonal phase, which split on passing into the modulated phase, are found to be inhomogeneously broadened. This is related quantitatively to sub-unit cell distortions brought about by Al–Si ordering. The same ordering is found to be related linearly to the decrease in widths of modes of other symmetries with annealing.

1. Introduction

Cordierite $(Mg, Fe^{2+})_2Al_4Si_5O_{18}$, is a framework silicate containing corner-sharing tetrahedra linked into six-membered rings. It occurs in at least two polymorphic forms. At high temperatures (greater than ≈1450 °C for the magnesium end member) the stable structure is hexagonal (space group P6/*mcc*), while the low-temperature form is orthorhombic (space group *Cccm*). Natural cordierites, with the single exception of indialite, are orthorhombic.

In the hexagonal phase of Mg cordierite the Al and Si atoms can have no long-range order, while within the orthorhombic structure stable at lower temperatures complete Al/Si ordering can be attained. Thus the hexagonal ↔ orthorhombic transformation is associated with Al/Si ordering. Natural cordierites are orthorhombic and appear to have fully ordered Al/Si distributions. Equilibrium hexagonal cordierite is difficult to produce artificially, since the melting temperature is only 5 K or so into its stability field.

More or less disordered Mg cordierite samples can, however, be produced metastably by annealing a glass of the correct composition at a temperature within the stability field of the ordered, orthorhombic form, followed by rapid quenching (Putnis 1980). The first

§ Now at: Department of Physics, University of Edinburgh, Mayfield Road, Edinburgh EH9 3JZ, UK.

0953-8984/90/306361 + 12 $03.50

cordierite to crystalise out is hexagonal. A 'modulated' phase appears at longer annealing times. This in turn transforms into the orthorhombic phase upon further annealing.

This is the fourth in a series of papers in which these various structural states obtained in the course of isothermal annealing are investigated and discussed.

In paper I (Putnis *et al* 1987), it was shown that the degree of Al–Si order is a continuous function of annealing time. In fact, the number of Al–O–Al bonds per formula unit N (= 3.3 for fully disordered, and = 0 for perfect order) obtained from ^{29}Si magic angle spinning NMR decreases linearly as the logarithm of annealing time. However, long-range displacive distortion appears suddenly in this system. This distortion can be measured by the splitting of the (211) peak in the hexagonal structure into the (131), (421) and (511) peaks of the orthorhombic structure (Miyashiro 1957):

$$\Delta = 2\theta_{131} - (2\theta_{511} - 2\theta_{421})/2 \tag{1}$$

which takes a maximum value of $\Delta_{max} = 0.25$. Paper I showed that $\Delta = 0$ not only in the hexagonal phase, but also in the modulated phase. Then, at the modulated → orthorhombic transition point, Δ jumps to the high value of 0.22, increasing only to 0.25 for fully ordered samples.

In paper II (Salje 1987), Salje defined two different order parameters to model the behaviour of isothermally annealed cordierite. Q_{od} governs the Al–Si ordering process and is defined as

$$Q_{od} = \sqrt{\langle\sigma\rangle} \tag{2}$$

where

$$\sigma = 1 - N/3.3 \tag{3}$$

is the short-range order parameter describing the topology of local bonding and $\langle \ldots \rangle$ indicates the thermodynamic average. Q describes the displacive distortions and is proportional to Δ. Both processes lead to the same symmetry reduction P6/mcc → Cccm, the active representation being E_{2g}. In the orthorhombic phase, in which $Q_{od} \neq 0$, $Q \neq 0$, it was proposed that there is bilinear coupling. In both of the other phases, $Q_{od} = Q = 0$. Since there was no abrupt change in local Al–Si order, however, a precursor order parameter $\tilde{Q}_{od}$ was defined:

$$\tilde{Q}_{od}^2 = \langle\sigma\rangle_{local}. \tag{4}$$

The subscript 'local' indicates that the spatial averaging is carried out on a much smaller scale than that indicated in the definition of Q_{od}.

With these definitions, papers I and II can be summarised schematically in the order parameter vector space; see figure 1.

Paper III (Güttler *et al* 1988) investigated the structural states of Mg cordierite on a local scale using infrared spectroscopy. By studying the line profiles of various absorption peaks, these authors showed that the phase transition between hexagonal and modulated cordierite was stepwise as predicted in paper II. It was also shown that the local structure of quenched, modulated cordierite was essentially equivalent to that of the orthorhombic phase.

McMillan *et al* (1985) have studied the sequence of structures obtained in the isothermal annealing of Mg cordierites using Raman spectroscopy before. From their results, it is clear that the most striking changes in the Raman spectrum with increasing annealing times are (i) the splitting of peaks, and (ii) the sharpening of lines. There was, however, no quantitative analysis in their work. In this paper, we have reinvestigated

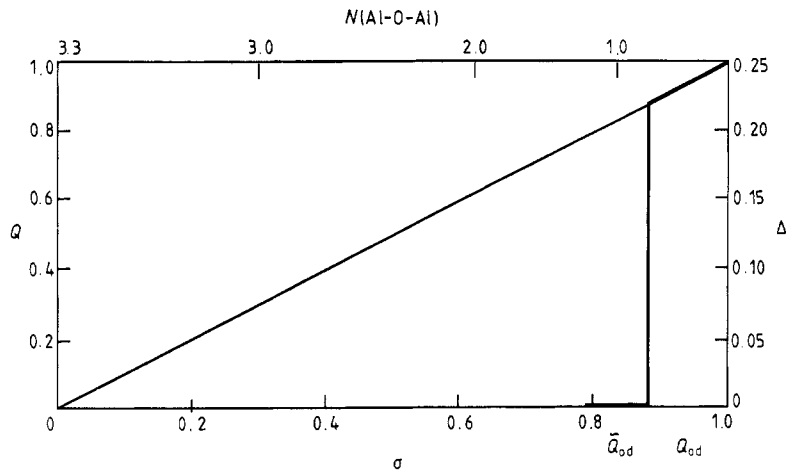

Figure 1. The order parameter vector space for Mg cordierite. The bold curve represents schematically the experimental data—Q_{od} being determined from NMR measurements of N(Al–O–Al) and Q being determined from the Miyashiro distortion index Δ. The actual position of the discontinuity varies somewhat with annealing temperature. The fine curve is the prediction of bilinear order parameter coupling theory with equal transition temperatures.

the Raman scattering of the various structural states to obtain quantitative results relating mode splitting and linewidths to the local behaviour of order parameters.

2. Experimental details and results

The samples used in our study were prepared in exactly the same way and from the same batch of starting glass material as that used in paper I. Small pieces ($\simeq 2$ mm $\times$ 2 mm $\times$ 1 mm each) of the glass of the right composition were placed in a platinum crucible and annealed in a constant temperature furnace for a specific length of time. A brief but fixed period was allowed to elapse after each sample was introduced into the furnace before the measurement of annealing time was started—this was necessary for the sample to reach annealing temperature. After the required annealing time, the Pt crucible containing the sample was dropped into water at room temperature.

Raman spectra were collected using a Coderg T-800 triple monochromator with spectral resolution between 0.8 and 1.6 cm^{-1}. A 3 W Ar^+ laser working at 514.5 nm was employed. The spectra of McMillan *et al* (1984) show that the most prominent peak in the hexagonal phase is centred at $\simeq$566 cm^{-1}; furthermore, this peak splits on passing from the hexagonal to the modulated structure. At a slightly higher frequency, centred at $\simeq$672 cm^{-1}, there is another mode which clearly grows in relative intensity and sharpens with increasing annealing. We therefore focused our attention on these two Raman modes in our investigation. The evolution of the 566 cm^{-1} peak with annealing time (annealing temperature = 1290 °C) is shown in figure 2, while the behaviour of the 672 cm^{-1} mode (annealing temperature = 1180 °C) is shown in figure 3.

Selected samples were cooled using either a home-made cold-finger liquid nitrogen cryostat or an Oxford Instruments continuous-flow liquid helium cold-finger cryostat.

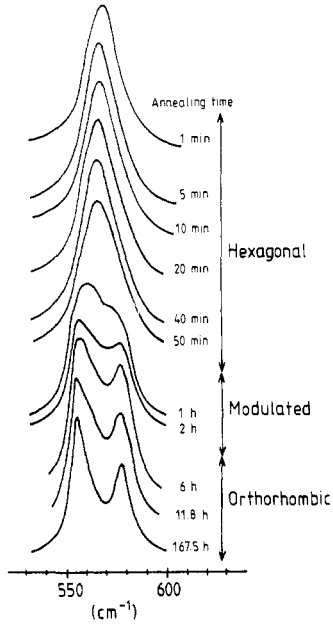

Figure 2. The evolution of the Raman spectrum of Mg cordierite in the 500–600 cm^{-1} region with increasing annealing time (annealing temperature = 1290 °C). The structural state of each sample according to the x-ray and NMR results of Putnis *et al* (1987) is also shown. Notice the sudden appearance of mode splitting at the point of the hexagonal → modulated transition.

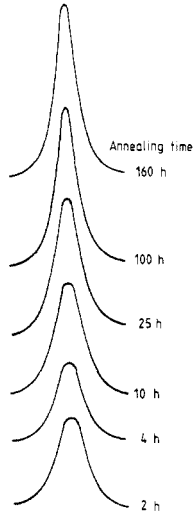

Figure 3. The evolution of the 672 cm^{-1} mode with annealing time (annealing temperature = 1180 °C). The peak sharpens considerably as the material becomes more ordered. This is a general feature of many other Raman modes in Mg cordierite.

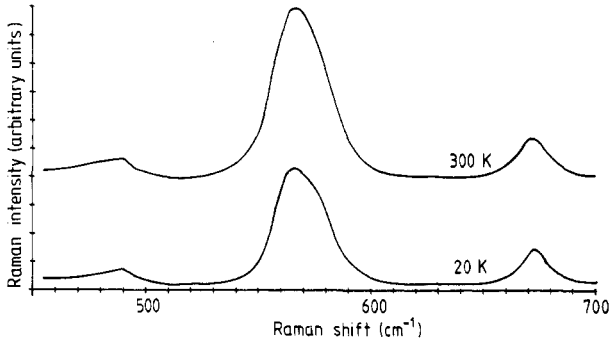

Figure 4. The effect of cooling. The sharpening of the peaks gives a measurement of the thermal contribution of the total linewidth. The existence of a second mode on the high-frequency side of the 566 cm^{-1} peak is also clearly seen. (The sample was annealed at 1180 °C for 6 h 40 min.)

This was to allow us to estimate the thermal contribution to line widths as well as confirm the existence of a weak mode close to the 566 cm^{-1} band. The effect of cooling on the hexagonal phase spectrum in the region of interest is shown in figure 4.

Table 1. The atomic positions in hexagonal cordierite determined by Dove *et al* (1990) using neutron powder diffraction.

Site symbol	Atom(s)	Positions
4c	Mg	$\frac{1}{3}, \frac{2}{3}, \frac{1}{4}$
6f	Al, Si [T_1]	$\frac{1}{2}, \frac{1}{2}, \frac{1}{4}$
12l	Al, Si [T_2]	0.372, 0.266, 0
24m	O_1	0.485, 0.349, 0.144
12l	O_2	0.230, 0.308, 0

3. Group theoretic analysis of vibrations

Hexagonal cordierite has space group symmetry P6/m*cc* ($Z = 2$). The atomic positions as determined by Dove *et al* (1990) are given in table 1, where T_1 and T_2 refer to the two kinds of tetrahedral sites in the unit cell (see Putnis 1980). Using the tables in Rousseau *et al* (1981), we can work out the zone-centre vibrational modes due to the occupation of these sites in P6/m*cc*. The results are as follows:

$$\text{Mg: } A_{2g} + A_{2u} + B_{1g} + B_{1u} + E_{1g} + E_{1u} + E_{2g} + E_{2u}$$

$$T_1\text{: } A_{2g} + A_{2u} + B_{1g} + B_{1u} + B_{2b} + B_{2u} + 2E_{1g} + 2E_{1u} + E_{2g} + E_{2u}$$

$$T_2\text{: } 2A_{1g} + A_{1u} + 2A_{2g} + A_{2u} + B_{1g} + 2B_{1u} + B_{2g} + 2B_{2u} + 2E_{1g} + 4E_{1u} + 4E_{2g} + 2E_{2u}$$

$$O_1\text{: } 3(A_{1g} + A_{1u} + A_{2g} + A_{2u} + B_{1g} + B_{1u} + B_{2g} + B_{2u}) + 6(E_{1g} + E_{1u} + E_{2g} + E_{2u})$$

$$O_2\text{: } 2A_{1g} + A_{1u} + 2A_{2g} + A_{2u} + B_{1g} + 2B_{1u} + B_{2g} + 2B_{2u} + 2E_{1g} + 4E_{1u} + 4E_{2g} + 2E_{2u}.$$

The total irreducible representation is therefore

$$\Gamma = 7A_{1g} + 5A_{1u} + 9A_{2g} + 7A_{2u} + 7B_{1g} + 9B_{1u} + 6B_{2g} + 8B_{2u} + 13E_{1g} + 17E_{1u} + 16E_{2g} + 12E_{2u}$$

of which

$$\Gamma_{ac} = A_{2u} + E_{1u}$$

$$\Gamma_{opt} = 7A_{1g} + 13E_{1g} + 16E_{2g} \quad \text{(raman active)}$$
$$+ 6A_{2u} + 16E_{1u} \quad \text{(infrared active).}$$

These results are identical with those obtained in paper III using correlation tables from

another source. The Raman tensors for the active modes are as follows (Hayes and Loudon 1978):

$$A_{1g} \quad \begin{pmatrix} a & 0 & 0 \\ 0 & a & 0 \\ 0 & 0 & b \end{pmatrix}$$

$$E_{1g} \quad \begin{pmatrix} 0 & 0 & 0 \\ 0 & 0 & d \\ 0 & e & 0 \end{pmatrix} \quad \begin{pmatrix} 0 & 0 & -d \\ 0 & 0 & 0 \\ -e & 0 & 0 \end{pmatrix}$$

$$E_{2g} \quad \begin{pmatrix} 0 & f & 0 \\ f & 0 & 0 \\ 0 & 0 & 0 \end{pmatrix} \quad \begin{pmatrix} f & 0 & 0 \\ 0 & -f & 0 \\ 0 & 0 & 0 \end{pmatrix}.$$

The active representation for the hexagonal → orthorhombic transition is E_{2g}. The E modes can all be expected to split on passing into the orthorhombic phase. Furthermore, one of the two E_{2g} scattering matrices contains diagonal components, so an intense mode that splits on passing from high to low symmetry (such as the mode at 566 cm^{-1}) is likely to be of this symmetry and can couple directly to either or both of the order parameters.

4. Order parameter dependence of mode splitting

The 566 cm^{-1} mode is the strongest mode in the Raman spectrum of the hexagonal phase, and is also the mode that splits most clearly as the annealing time increases. The discussion at the end of the last section then suggests that this is probably an E_{2g} mode. In all cases studied, the splitting occurs at precisely the point when the synchrotron and TEM results show that the *modulated* phase appears (see figure 2). Further annealing does not bring about any more qualitative changes to the Raman spectrum (cf McMillan *et al* 1984). In figure 2, we see that once the splitting has occurred, further annealing only brings about sharpening of the individual peaks (and a slight but important increase in splitting; see below).

From group theory, splitting of E modes is associated with the change from hexagonal to orthorhombic symmetry. We must therefore conclude that on the Raman length scale (a few unit cells; see, e.g., Yacoby 1978), the quenched modulated phase is already orthorhombic. This agrees with the IR results of Güttler *et al* in paper III, who reached a similar conclusion for the structure of the quenched modulated phase on the IR length scale.

The emergence of overall, macroscopic orthorhombic symmetry is associated with the activation of the displacive order parameter Q (see section 1 and figure 1). The vibrational spectroscopy results therefore motivate us to define another precursor order parameter $\tilde{Q}$ (analogous to the $\tilde{Q}_{od}$ that was defined in equation (4)) which is the local version of Q. The transition from hexagonal to modulated cordierite is then associated with a stepwise change in $\tilde{Q}$ which shows up experimentally as the sudden emergence of mode splitting in the Raman spectrum.

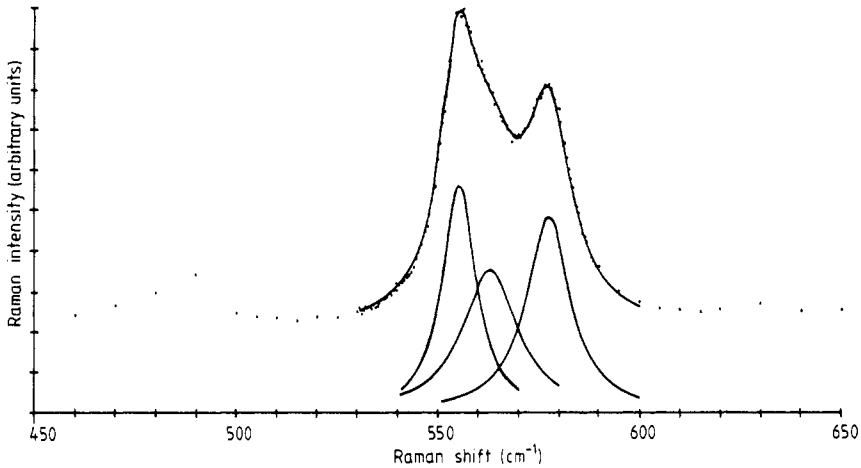

Figure 5. A typical fitting (full curve) of three modes to the data (dots) between 530 and 600 cm^{-1}. The three modes used for the fit are also shown individually. The central mode is found to be present even in fully orthorhombic samples, and therefore should not be seen as due to residual hexagonal material.

The exact mode splitting has been determined for all the samples studied by fitting spectra to n phonon profiles of the form

$$I(\omega) = \mathrm{Im} \sum_{i=1}^{n} \frac{C_i}{\Omega_i^2 - \omega^2 + i\omega\Gamma_i} \tag{5}$$

It was found that *three* peaks were in fact present between 530 cm^{-1} and 600 cm^{-1}. The typical fit obtained is shown in figure 5. The original 566 cm^{-1} peak in hexagonal cordierite is split into two components centred at $\simeq$557 cm^{-1} and 578 cm^{-1}, while a third peak is centred round 564 cm^{-1}. It is tempting to associate the 564 cm^{-1} peak with residual hexagonal phase in the modulated structure. This, however, is untenable, because this mode was found to be still strongly present in samples that were definitely orthorhombic and almost fully ordered. We must therefore conclude that most of the intensity centred round 564 cm^{-1} is due to a *bona fide* mode belonging to the orthorhombic symmetry. This, of course, does not preclude some contribution from residual hexagonal material, but this contribution will be hard to separate out. Arguments in the next section suggest that the two peaks resulting from the splitting of the parent 566 cm^{-1} mode should be separated by $\simeq$20 cm^{-1}, which is indeed the separation between the outer two peaks used to fit our data.

This splitting can be related quantitatively to the relevant order parameters by using the theory developed in detail in Petzelt and Dvorak (1976).

Consider the phonon contribution to the free energy of the parent (high-symmetry) phase. In the quasi-harmonic approximation, this can be written as

$$\Delta G_{\mathrm{ph}} = \tfrac{1}{2} \sum_{i=1}^{n} \chi_i^{-1} Q_1^2 + \ldots + e_i Q_i F \tag{6}$$

where Q_i is the ith normal coordinate and χ_i the associated susceptibility

$$\chi_i = m_i^{-1} \omega_i^{-2}. \tag{7}$$

For infrared spectroscopy, e_i is the effective charge of the ith mode, which couples to

the field F, the electric field of the incident radiation. In order to ensure that equation (6) retains the same form for Raman spectroscopy, we define

$$e_i = \delta\chi_i^{\mathrm{E}}(\omega_{\mathrm{L}})/Q_i \tag{8}$$

where $\chi_i^{\mathrm{E}}(\omega_{\mathrm{L}})$ is the laser frequency electric susceptibility. With this definition of e_i, the 'effective Raman field' F is then the total change in $\chi^{\mathrm{E}}(\omega_{\mathrm{L}})$ per unit scattering cross section (see Petzelt and Dvorak (1976) for details).

Below T_{c}, the normal modes of the parent phase are no longer normal, and can interact bilinearly. The phonon contribution to the free energy now becomes

$$\Delta G_{\mathrm{ph}} = \tfrac{1}{2}\sum_{ij}\alpha_{ij}^{-1}Q_iQ_j + \ldots + \sum_i e_iQ_iF \tag{9}$$

where $\alpha_{ii} = \chi_i^{-1} + \delta\alpha_{ii}(T)$ and $\alpha_{ij}(T)$ are coupling coefficients. All the $\delta\alpha_{ii}(T)$ and $\alpha_{ij}(T)$ decrease continuously to zero on approaching T_{c} and are therefore functions of the order parameter, Q. In the case of a non-degenerate mode and to the lowest order $\delta\alpha_{ij} \propto Q^2$. It can also be shown that $\delta\omega_i^2 \propto \delta\chi_i^{-1} \simeq \delta\alpha_{ij}$, so $\delta\omega_i^2 \propto Q^2$.

The case of degeneracy introduces new types of coupling terms into the free-energy expression. We will denote the d-fold-degenerate components of the mode under investigation by $Q_1, \ldots, Q_{\mathrm{d}}$. There can now be diagonal as well as non-diagonal coupling among these components. In the specific case of two-fold degeneracy (as in the $\mathrm{E}_{2\mathrm{g}}$ mode of hexagonal cordierite), the two possible diagonal terms are $\alpha_+(Q_1^2 + Q_2^2)$ and $\alpha_-(Q_1^2 - Q_2^2)$. The α_+ term leads to a change in the 'centre of gravity' of the squared mode frequency which is again proportional to Q^2 in the lowest order. In a case where the degeneracy is not removed through a phase transition, $\alpha_- = 0$. When the degeneracy is lifted and the mode splits in the low symmetry phase, $\alpha_- \neq 0$, and Petzelt and Dvorak showed that

$$\delta\omega_{12}^2 = \tilde{\omega}_1^2 - \tilde{\omega}_2^2 \propto \alpha_- \tag{10}$$

and that

$$\alpha_- \propto Q^u \tag{11}$$

where in most cases $u = 1$ or 2, the actual value being determined by experiment. For hard modes we can, to a very good approximation, write

$$\delta\omega_{12}^2 = \tilde{\omega}_1^2 - \tilde{\omega}_2^2 = (\tilde{\omega}_1 + \tilde{\omega}_2)(\tilde{\omega}_1 - \tilde{\omega}_2) \simeq (\tilde{\omega}_1 - \tilde{\omega}_2) \tag{12}$$

so

$$\delta\omega_{12} = \tilde{\omega}_1 - \tilde{\omega}_2 \propto Q^u. \tag{13}$$

In the case of cordierite, there are two order parameters of the same symmetry, so we have (see Güttler *et al* 1988)

$$\delta\omega_{12} = \begin{cases} AQ_{\mathrm{od}}^u + BQ^u & \text{(orthorhombic)} \qquad (14a) \\ A\tilde{Q}_{\mathrm{od}}^u + B\tilde{Q}^u & \text{(modulated).} \qquad (14b) \end{cases}$$

There is no abrupt change of Al/Si order on going from the hexagonal phase to the modulated phase and then to the orthorhombic phase (see figure 1), but the mode splitting does appear abruptly at the hexagonal → modulated transition (figure 2). This implies that $A = 0$ in equation (14), giving us

$$\delta\omega_{12} = BQ^u. \tag{15}$$

The value of the exponent u can be found by plotting the mode splitting measured

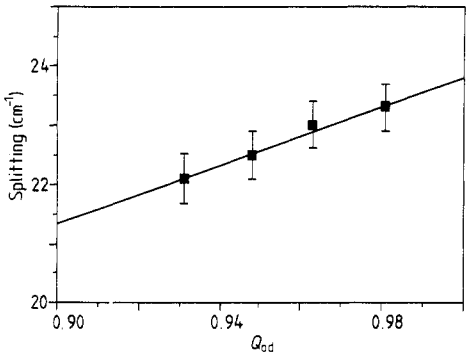

Figure 6. The splitting of the 566 cm^{-1} mode observed in four orthorhombic samples (annealing temperature 1290 °C) with different degrees of Al/Si order. The best straight line shown extrapolates to a very small value at $Q_{od} = 0$. Previous work shows that $Q \propto Q_{od}$ in the orthorhombic phase; this plot therefore suggests that the mode splitting is a direct measure of Q.

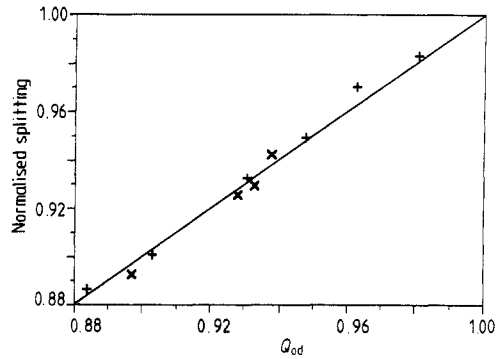

Figure 7. The normalised splittings of the 566 cm^{-1} mode from samples run at two different annealing temperatures (+ = 1290 °C; × = 1180 °C). The two data points for 1290 °C with lowest Q_{od} and all the data points for 1180 °C are from samples with *modulated* structures. This shows that $\tilde{Q} \propto \tilde{Q}_{od}$ on the local scale.

in orthorhombic samples against Q_{od}. This is done in figure 6, according to which $\delta\omega_{12} \propto Q_{od}$. We know from the work of Putnis *et al* (1987) that $Q \propto Q_{od}$ in the orthorhombic phase (see figure 1). Taking these two proportionalities together, we see that $u = 1$, i.e. the normalised mode splitting $\delta\omega_{12}/\delta\omega_{12}^{max}$ is a direct measure of Q and $\tilde{Q}$. We can therefore use the mode splitting to determine the relationship between $\tilde{Q}$ and $\tilde{Q}_{od}$ in the modulated phase.

The normalised mode splitting for a number of samples with modulated structures for two different annealing temperatures is plotted against $\tilde{Q}_{od}$ in figure 7. The normalised values of the orthorhombic samples taken from figure 7 are also included. A straight proportionality is observed for all the data points taken together. Clearly, the proportionality between Q and Q_{od} extends to the local scale for the quenched modulated phase. Therefore the coupling between $\tilde{Q}$ and $\tilde{Q}_{od}$ is again bilinear.

The results presented in this section show that Raman spectroscopy is sensitive to order parameter behaviour on a local scale, and can provide information that cannot be easily obtained by any other experimental techniques. In this case, we have been able to show that the proportionality of Q and Q_{od} in the orthorhombic phase of Mg cordierite extends into the modulated phase on a local scale as proportionality between $\tilde{Q}$ and $\tilde{Q}_{od}$.

5. Inhomogeneous broadening in the hexagonal phase

The intensity distribution round 566 cm^{-1} in the hexagonal phase is asymmetric. This becomes very clear at low temperatures—see figure 4. Another mode of medium intensity is present on the high-frequency side of the main 566 cm^{-1} mode. This mode, with a centre at $\simeq$576 cm^{-1}, was not reported by McMillan *et al* (1984). There is no evidence of a mode in this position in the modulated or orthorhombic spectra.

The width of the 566 cm^{-1} mode was found by doubling the half width obtained from data points with $\omega < 566\,cm^{-1}$ to eliminate the effect of the side mode. This 'symmetrised

width' Γ is much larger than can be accounted for by normal thermal broadening (multiphonon processes). This latter contribution should decrease to zero at helium temperatures. Low-temperature runs indicate (figure 4) that the thermal contribution to Γ is $\Gamma_{th} \simeq 6\ cm^{-1}$. The slit width of the spectrometer Γ_s ($\simeq 1\ cm^{-1}$) should also be subtracted. We thus obtain $\Gamma_{566} = \Gamma - \Gamma_{th} - \Gamma_s$, the deconvoluted residual linewidth. These values are plotted against the logarithm of annealing time in figure 8. It is known that a finely divided powder sample could give large residual linewidths. The particulate size needed, however, is of the order of a few Å. Low-resolution TEM images show that our method of sample preparation gives grain sizes of the order of micrometres. Another explanation must therefore be sought.

Large residual linewidths have been observed before in the Na–K feldspar anorthoclase (Salje 1986). The 514 cm^{-1} and 473 cm^{-1} modes in this material show residual linewidths of 10 cm^{-1} and 16 cm^{-1} at 0 K respectively, values comparable to that obtained for the shortest annealing times used in our cordierite experiments. In the case of anorthoclase, the residual linewidth was interpreted as being due to inhomogeneous broadening related to static structural distortions. Na/K site ordering distorts the Si–Al–O framework because of inequivalent alkali positions. The residual broadening of the Raman modes at 0 K is then a measure of the width of the statistical distribution of the local distortions.

The interpretation of the residual width in the case of hexagonal cordierite is similar. The distribution of Al/Si atoms on the two types of tetrahedral sites (see section 3) is such that accurate hexagonal symmetry should only be obtainable with complete disorder. This is associated with an average of $N = 3.3$ Al–O–Al linkages per formula unit. However, even for an annealing time as short as 1 min, the degree of local order is already very high, with $N \simeq 1.5$ and the short-range order parameter $\sigma \simeq 0.6$ (values for $T_{anneal} = 1290$ °C). Locally, say on the scale of the T_2 rings, the symmetry cannot therefore be hexagonal. The local distortions, however, could be so arranged on the scale observable by x-ray techniques that they cancel out to give overall hexagonal symmetry. Raman spectroscopy, on the other hand, is a very local probe and sees the static distribution of local distortions.

We can postulate that in perfectly disordered hexagonal cordierite there is a Raman-active mode of E_{2g} symmetry at 566 cm^{-1} of normal width (say 6 cm^{-1} at room temperature), probably associated with Si–O–Si bending. The distribution of local static distortions brought about by ordering gives a distribution of modes split to varying degrees, but never more than $\delta\omega_{max} \simeq 24\ cm^{-1}$ (the value observed for a fully ordered orthorhombic material). The width of the peak at 566 cm^{-1} for hexagonal cordierite with $\sigma \geqslant 0.6$ is then the result of convoluting together the contributions from tetrahedra distorted locally to varying degrees.

The symmetrised width of the inhomogeneously broadened 566 cm^{-1} peak corrected for thermal and instrumental contributions is replotted in figure 9 against the short-range order parameter σ. Note that there is a linear region; this extrapolates to $\Gamma_{566} \simeq 2\ cm^{-1}$ at $\sigma = 0$. This confirms that the observed width is due to distortions introduced by Al–Si ordering. Furthermore, our interpretation is that the composite width of the peak is built up from contributions from scattering units distorted locally to varying extents. This plot then shows that these local distortions are coupled to σ. The existence of such coupling is necessary for the hexagonal $\rightarrow$ modulated transition to be stepwise. The discontinuous nature of the transition is, of course, also evident from the plots in figures 9 and 10—there is departure from linearity close to σ_{crit}, where the rise in width is much more rapid. From figure 10, it appears reasonable to suggest that just prior to

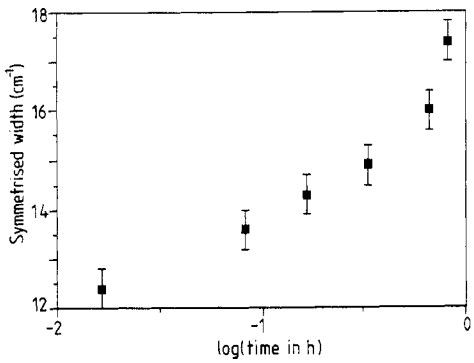

Figure 8. The residual width of the 566 cm^{-1} peak in hexagonal cordierite plotted against the logarithm of the annealing time (annealing temperature = 1290 °C). Note that log(time) = 0 corresponds to the transition point to the modulated phase for this annealing temperature.

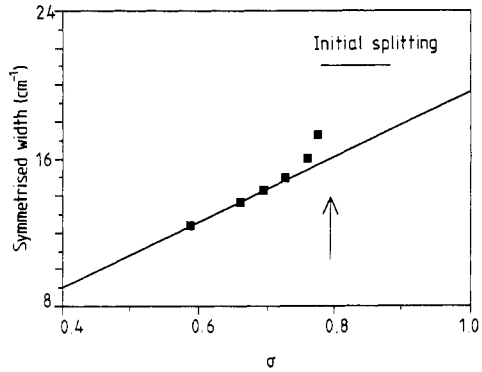

Figure 9. The symmetrised width of the 566 cm^{-1} peak in hexagonal cordierite corrected for thermal and spectrometer contributions plotted against the short-range order parameter. The linear portion extrapolates to 2 cm^{-1} at $\sigma = 0$. The rapid rise observed near $\sigma = 0.8$ confirms the stepwise character of the hexagonal → modulated transition. The mode splits on entering the modulated phase; the initial value of this splitting is indicated.

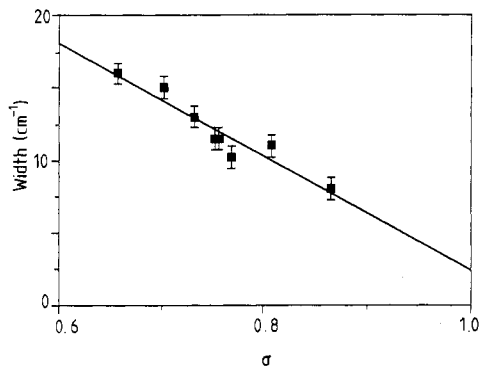

Figure 10. The width of the 672 cm^{-1} mode decreases linearly with increasing short-range order parameter σ. For $\sigma = 1$ we find a small width of 2.4 cm^{-1}. Remembering that $\sigma = 1 - N/3.3$, we see that the width of this mode is clearly a sensitive probe of local bond topology.

the transition, the symmetrised width will be very close to the observed value of the mode splitting just after the transition has occurred ($\simeq 21$ cm^{-1}).

6. Disorder broadening

We have also investigated the behaviour of the mode in Mg cordierite at 672 cm^{-1}, which does not appear to split on the appearance of local orthorhombic symmetry in the modulated phase. It increases in intensity relative to the band(s) around 566 cm^{-1} with increasing annealing time. Moreover, figure 3 shows clearly that this mode sharpens up considerably with annealing. Cooling to liquid helium temperatures (figure 4) showed that the thermal contribution to this mode is $\Gamma_{th} \simeq 4$ cm^{-1}. The spectrometer contribution

is $\Gamma_s \simeq 1\ cm^{-1}$. These are subtracted from the measured full width half heights to obtain the intrinsic widths Γ_{672}.

The values obtained are plotted as a function of the short-range-order parameter σ in figure 10. It is immediately apparent that the intrinsic width of this mode decreases linearly as Al/Si ordering progresses. When the material is fully ordered and there are no Al–O–Al linkages, and Γ_{672} extrapolates to a small value ($\simeq 2\ cm^{-1}$).

The decrease of peak width more or less linearly with σ is in fact a feature not confined to the 672 cm^{-1} mode. For example, it can be seen from figure 2 that the two individual peaks derived from the 566 cm^{-1} mode themselves sharpen up with increasing annealing time. Conversely, the increase in width as one moves away from the ideal orthorhombic phase ($\sigma = 1$) is a reflection of the increasing degree of local disorder, i.e. there is a strong density of states contribution to the width of Raman modes. The same general observation can be made concerning the IR data of Güttler *et al* (1988).

Acknowledgments

WCKP thanks the Croucher Foundation (HK) and St John's College (Cambridge) for financial support for this work.

References

Dove M T, Putnis A, David W I F and Harrison W T A 1989 to be published
Güttler B, Salje E and Putnis A 1988 *Phys. Chem. Minerals* **16** 365
Hayes W and Loudon 1978 *Scattering of Light by Crystals* (New York: Academic)
McMillan P, Putnis A and Carpenter M A 1985 *Phys. Chem. Minerals* **10** 256
Miyashiro A 1957 *Am. J. Sci.* **255** 43
Petzelt J and Dvorak V 1976 *J. Phys. C: Solid State Phys.* **21** 1571
Putnis A 1980 *Nature* **287** 128
Putnis A, Salje E, Redfern S A T, Fyfe C A and Strobl H 1987 *Phys. Chem. Minerals* **14** 446
Rousseau K L, Bauman R P and Porto S P S 1981 *J. Raman. Spectrosc.* **10** 253
Salje E 1986 *Phys. Chem. Minerals* **13** 340
—— 1987 *Phys. Chem. Minerals* **14** 455
Yacoby Y 1978 *Z. Phys.* B **31** 275